

## Measurement-only topological quantum computation without forced measurements

This content has been downloaded from IOPscience. Please scroll down to see the full text.

2016 New J. Phys. 18 123027

(<http://iopscience.iop.org/1367-2630/18/12/123027>)

View [the table of contents for this issue](#), or go to the [journal homepage](#) for more

Download details:

IP Address: 130.132.173.98

This content was downloaded on 23/01/2017 at 20:14

Please note that [terms and conditions apply](#).

You may also be interested in:

[Preparing topologically ordered states by Hamiltonian interpolation](#)

Xiaotong Ni, Fernando Pastawski, Beni Yoshida et al.

[A family of stabilizer codes for  \$D\(\mathbb{Z}\_2\)\$  anyons and Majorana modes](#)

James R Wootton

[Introduction to topological superconductivity and Majorana fermions](#)

Martin Leijnse and Karsten Flensberg

[Physical implementation of a Majorana fermion surface code for fault-tolerant quantum computation](#)

Sagar Vijay and Liang Fu

[Fractionalized flux, Majorana fermions and non-Abelian anyons in topological superfluid on optical lattices](#)

Ya-Jie Wu and Su-Peng Kou

[Globally symmetric topological phase: from anyonic symmetry to twist defect](#)

Jeffrey C Y Teo

[Designer non-Abelian anyon platforms: from Majorana to Fibonacci](#)

Jason Alicea and Ady Stern

[An efficient magic state approach to small angle rotations](#)

Earl T Campbell and Joe O'Gorman

[Generalized cluster states based on finite groups](#)

Courtney G Brell



## PAPER

## Measurement-only topological quantum computation without forced measurements

## OPEN ACCESS

## RECEIVED

9 October 2016

## REVISED

28 November 2016

## ACCEPTED FOR PUBLICATION

30 November 2016

## PUBLISHED

22 December 2016

Original content from this work may be used under the terms of the [Creative Commons Attribution 3.0 licence](#).

Any further distribution of this work must maintain attribution to the author(s) and the title of the work, journal citation and DOI.

Huaixiu Zheng<sup>1,2</sup>, Arpit Dua<sup>1,2</sup> and Liang Jiang<sup>1,2</sup><sup>1</sup> Departments of Applied Physics and Physics, Yale University, New Haven, CT, USA<sup>2</sup> Yale Quantum Institute, Yale University, New Haven, CT 06520, USAE-mail: [huaixiu.zheng2013@gmail.com](mailto:huaixiu.zheng2013@gmail.com) and [liang.jiang@yale.edu](mailto:liang.jiang@yale.edu)**Keywords:** topological quantum computation, Majorana fermions, parafermions, measurement-based braiding, quantum information**Abstract**

We investigate the measurement-only topological quantum computation (MOTQC) approach proposed by Bonderson *et al* (2008 *Phys. Rev. Lett.* **101** 010501) where the braiding operation is shown to be equivalent to a series of topological charge ‘forced measurements’ of anyons. In a forced measurement, the charge measurement is forced to yield the desired outcome (e.g. charge 0) via repeatedly measuring charges in different bases. This is a probabilistic process with a certain success probability for each trial. In practice, the number of measurements needed will vary from run to run. We show that such an uncertainty associated with forced measurements can be removed by simulating the braiding operation using a fixed number of three measurements supplemented by a correction operator. Furthermore, we demonstrate that in practice we can avoid applying the correction operator in hardware by implementing it in software. Our findings greatly simplify the MOTQC proposal and only require the capability of performing charge measurements to implement topologically protected transformations generated by braiding exchanges without physically moving anyons.

**1. Introduction**

Anyons are excitations of topological phases and exhibit exotic exchange statistics [1, 2], different from either fermions or bosons. In particular, non-Abelian anyons which obey noncommutative exchange statistics can be used to encode and process quantum information in the associated topological degenerate subspace for topological quantum computation (TQC). Such a subspace is characterized by topology, and is robust against local perturbations. This intrinsic error-protection holds great promise for fault-tolerant TQC and has triggered a lot of interest in searching for non-Abelian anyons.

Examples of non-Abelian anyons with realistic proposals of physical setups include Majorana [3–5] and parafermion zero modes [6]. Several experiments have found convincing evidence of the existence of Majorana zero modes in systems of semiconductor nanowires in proximity to a superconductor [7–11] and magnetic ad-atomic chains placed on the surface of a superconductor [12]. Recently, the characteristic exponential energy splitting of Majorana zero modes has been observed in proximity-induced superconducting Coulomb islands [13]. Such an exponential protection implies that quantum information can be encoded in the degenerate topological states in a non-local manner. Rotations on the logical space can be performed through braiding exchanges of Majorana modes, which only depend on the topology of the braiding path and are robust against local noise [1]. However, the set of operations is limited to Clifford gates and is not complete for universal quantum computation.

$\mathbb{Z}_N$  parafermion zero modes [6, 14] are generalizations of Majorana fermions (MFs) which correspond to the case  $N = 2$ . There have been several proposals to realize parafermions using quantum Hall states [15–20] and coupled wires [21–23] all of which involve strong electron–electron interactions in some form. In addition to the proposals in condensed matter settings, twist defects [24] introduced in the  $\mathbb{Z}_N$  toric code model have a quantum dimension of  $\sqrt{N}$  and behave as parafermions for general  $N$  [25–27]. Compared to MFs, parafermions provide a denser set of qudit rotations. Recently, a 2D lattice model of  $\mathbb{Z}_3$  parafermions is shown to support

more exotic Fibonacci anyons [28] which enable the universal set of gates. Therefore, parafermions are computationally more powerful and could potentially lead to the solution for universal TQC [29].

The exciting progress of experiments and theoretical ideas around MFs and parafermions motivates us to go beyond how to search for those exotic anyons and look into how to manipulate them for the purpose of (1) demonstrating non-Abelian exchange statistics as a short-term mission and (2) implementing quantum algorithms with topological quantum gates as a long-term goal. Traditional approach of TQC involves encoding in the topological protected subspace, initialization and readout of the logical qubits via measurements of topological charges, and braiding operations to implement the quantum gates by slowly moving anyons around each other. Braiding has to be slow enough compared to the time scale set by the energy gap to avoid exciting quasiparticles, and fast enough compared to the time scale set by the residual energy splitting between topological degenerate states [30]. This makes braiding a challenging task.

Alternatively, braiding can be done using either interaction-based proposals [31, 32] or a measurement-only approach [33–35] without physically moving anyons. These two approaches are shown to be equivalent [36] and they can avoid diabatic errors associated with moving anyons. In particular, measurement-only approach will allow us to concentrate on improving measurement fidelity alone because that is the only type of operation required for MOTQC in order to initialize, braid and readout topological qubits. However, the MOTQC proposal uses a series of topological charge forced measurements to simulate braiding. Each forced measurement is a probabilistic ‘repeat-until-success’ process, and hence has an inherent uncertainty with respect to the number of operations. This poses a challenge to synchronize the clock for computations running in parallel.

In this paper, we propose a forced-measurement-free measurement-based braiding (FMF-MBB) protocol. Each braiding exchange can be simulated by performing three measurements supplemented by a correction operator. Using the examples of MFs and parafermions, we show that the correction operator compensates for charge transfers among anyons occurred during the three measurements. Furthermore, we demonstrate that we can apply the correction operator in software which greatly simplifies the protocol. We show explicitly how to apply the FMF-MBB protocol to the demonstration of braiding statistics and MOTQC.

## 2. MBB without forced measurements

### 2.1. Diagrammatic representation

Following [33, 36–40], we employ a diagrammatic representation of anyonic states and operators to describe a general anyon model. This representation encapsulates the topological properties of anyons independent of specific physical model. In general, an anyon model is defined by (1) a set  $\mathcal{C}$  of topological charges  $a, b, c, \dots \in \mathcal{C}$  carried by anyons, (2) fusion rules specifying how topological charges are splitted or combined, and (3) braiding rules specifying what happens to the anyonic state once two anyons exchange positions. There is a unique vacuum charge  $I$  which has trivial fusion and braiding rules. For each charge  $a$ , there exists a unique conjugate charge  $\bar{a}$  which can be generated from vacuum  $I$  together with  $a$ . The associative fusion algebra defines the fusion rules as

$$a \times b = \sum_{c \in \mathcal{C}} N_{ab}^c c, \quad (1)$$

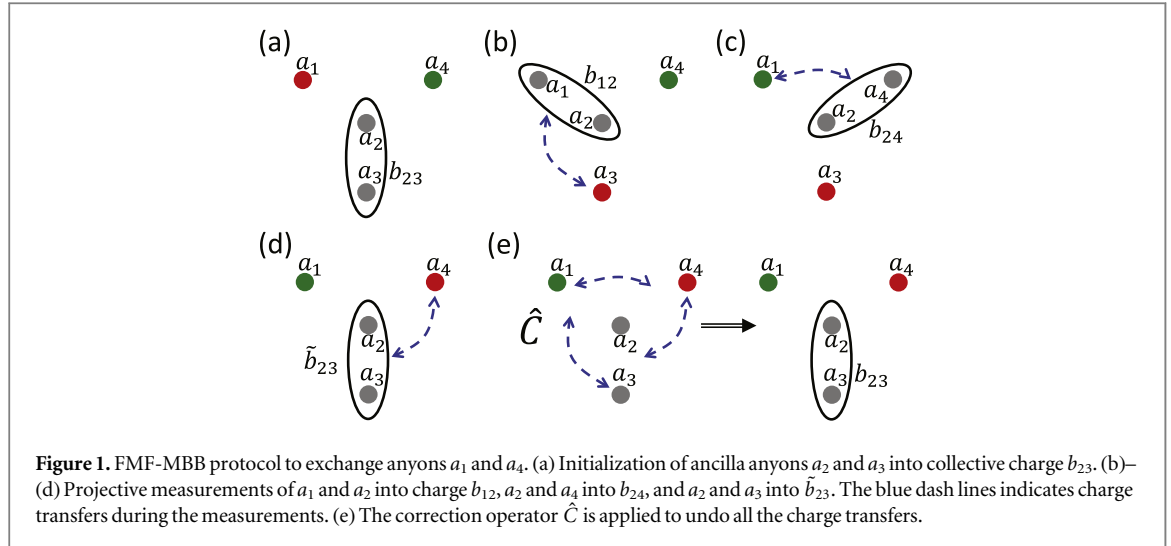
where the fusion multiplicity  $N_{ab}^c$  specifies the number of possible ways for charges  $a$  and  $b$  to fuse into charge  $c$ . The associated fusion and splitting Hilbert spaces  $V_{ab}^c$  and  $V_c^{ab}$  have the same dimension of  $N_{ab}^c$ . The states in fusion and splitting spaces can be represented by trivalent vertices

$$(d_c/d_a d_b)^{1/4} \begin{array}{c} c \\ \mu \\ \swarrow \quad \searrow \\ a \quad b \end{array} = \langle a, b; c, \mu | \in V_{ab}^c, \quad (2)$$

$$(d_c/d_a d_b)^{1/4} \begin{array}{c} a \quad b \\ \swarrow \quad \searrow \\ \mu \\ c \end{array} = |a, b; c, \mu \rangle \in V_c^{ab}, \quad (3)$$

where  $d_a$  is the quantum dimension of charge  $a$  and  $\mu = 1, 2, \dots, N_{ab}^c$  is the vertex label of basis. Most anyon models of physical interest and which are the ones we will consider have no fusion multiplicity, i.e.,  $N_{ab}^c = 0$  or 1, and therefore we will leave the vertex label  $\mu$  implicit hereafter. The state space involving more than one fusion or splitting obeys associativity determined by  $F$ -moves

$$\begin{array}{c} a \quad b \quad c \\ \swarrow \quad \searrow \\ e \\ \swarrow \quad \searrow \\ d \end{array} = \sum_f [F_d^{abc}]_{ef} \begin{array}{c} a \quad b \quad c \\ \swarrow \quad \searrow \\ f \\ \swarrow \quad \searrow \\ d \end{array}, \quad (4)$$



$$\begin{array}{c} a \\ \uparrow \\ c \end{array} \begin{array}{c} b \\ \uparrow \\ d \end{array} = \sum_f [F_{cd}^{ab}]_{ef} \begin{array}{c} a \\ \uparrow \\ c \end{array} \begin{array}{c} b \\ \uparrow \\ d \end{array} \quad (5)$$

where  $[F_{cd}^{ab}]_{ef} = \sqrt{\frac{d_e d_f}{d_a d_d}} [F_f^{ceb}]_{ad}^*$ . The counter-clockwise braiding operator can be represented diagrammatically

$$R_{ab} = \begin{array}{c} a \\ \nearrow \\ b \end{array} = \sum_c \sqrt{\frac{d_c}{d_a d_b}} R_c^{ab} \begin{array}{c} b \\ \nearrow \\ c \end{array} \begin{array}{c} a \\ \searrow \\ b \end{array} \quad (6)$$

where  $R_c^{ab}$  is the phase acquired after exchanging charges  $a$  and  $b$  which fuse together into charge  $c$ .

In this paper, we consider projective measurements of topological charges and physical examples include interferometry measurements [1, 39, 41–43], topological blockade readout of topological charge [44], magnetic flux controlled parity readout using a top-transmon system [30], and electric charge sensing using a quantum point contact or a quantum dot [45]. In the diagrammatic representation, the projector of two anyons with charges  $a_1$  and  $a_2$  projected onto collective charge  $b_{12}$  is given by

$$\Pi_{b_{12}}^{(12)} = \sqrt{\frac{d_{b_{12}}}{d_{a_1} d_{a_2}}} \begin{array}{c} a_1 \\ \nearrow \\ b_{12} \end{array} \begin{array}{c} a_2 \\ \searrow \\ b_{12} \end{array} \quad (7)$$

## 2.2. FMF-MBB protocol

The key insight of the MOTQC protocol is to teleport anyonic state via projective measurements [33]. As shown in figure 1(a), one can first initialize the ancilla anyons  $a_2$  and  $a_3$  into the collective charge  $b_{23}$ . Then, one can perform a projective measurement of the collective charge  $b_{12}$  of  $a_1$  and  $a_2$  (figure 1(b)). It is apparent that anyonic state encoded in  $a_1$  is teleported to  $a_3$  if  $b_{12} = b_{23}$ . In the case that  $b_{12} \neq b_{23}$ , one can go back to the initialization step and then measure  $b_{23}$  and then  $b_{12}$  again. Such a process can be repeated until the desired outcome  $b_{12} = b_{23}$  is obtained. This is the so-called forced measurement [33].

In general, without imposing forced measurements, at each step in figures 1(b)–(d) there will be charge transfers between anyons [30, 36] in addition to the anyonic state teleportation. This is the essence of our FMF-MBB protocol: we accept and keep track of the measurement results we obtain in figures 1(b)–(d), and supplement the final state with a correction operation to undo the charge transfers as shown in figure 1(e). The resulting state is the same as the initial state in figure 1(a) except that  $a_1$  and  $a_4$  are exchanged. Using equation (7), we can write down the product of three-projective-measurement (TPM) operator  $\hat{M}_{1,4,23}$  describing the projectors in figures 1(b)–(d) and  $\Pi_{b_{23}}^{(23)}$

$$\hat{M}_{1,4,2,3} \Pi_{b_{23}}^{(2,3)} = \Pi_{\tilde{b}_{23}}^{(2,3)} \Pi_{b_{24}}^{(2,4)} \Pi_{b_{12}}^{(1,2)} \Pi_{b_{23}}^{(2,3)}$$

$$= \mathcal{N}_1 \left[ \text{Diagram 1} \right] = \mathcal{N}_1 \left[ \text{Diagram 2} \right], \tag{8}$$

where  $\mathcal{N}_1$  is the normalization factor. Note that  $\Pi_{b_{23}}^{(2,3)}$  is not part of the TPM operator.

To further proceed with the calculation, it is essential to restrict ourselves to the case that *the intermediate collective charges*  $b_{23}, b_{12}, b_{24}$  and  $\tilde{b}_{23}$  are Abelian; otherwise the resulting operation will not be unitary and hence can not simulate braiding exchange [36]. This includes the Ising and  $\mathbb{Z}_N$  parafermion models but not the Fibonacci anyon model. Using the identities defined by *F*-moves in equations (4) and (5) and the Abelian-ness of  $b_{12}$  and  $b_{24}$ , we can move *A*' and *D*' to merge with *D* and *A* respectively, and there is only an additional phase factor

$$\hat{M}_{1,4,2,3} \Pi_{b_{23}}^{(2,3)} = \mathcal{N}_2$$

$$\tag{9}$$

where  $g = b_{12} \times \bar{b}_{24}$  and  $a_5 = a_4 \times a_2 \times a_3$ . Using equation (5), we can rewrite equation (9) as

$$\hat{M}_{1,4,2,3} \Pi_{b_{23}}^{(2,3)} = \mathcal{N}_3$$

$$\tag{10}$$

where  $h = \tilde{b}_{23} \times \bar{b}_{23}$ . Equation (10) provides a clear physical picture: compared to the forced measurement protocol, there are also charge transfers during the measurements in figures 1(b)–(d). These charge transfers are encoded in two processes in equation (10), namely exchange of Abelian charge  $g$  between  $a_1$  and  $a_4$ , and exchange of charge  $h$  between  $(a_2, a_3)$  and  $(a_1, a_4)$ .

After further manipulations utilizing the identities in equations (4)–(6),  $\hat{M}_{1,4,2,3}$  is brought into a form close to the desired braiding-exchanged result

$$\hat{M}_{1,4,2,3} \Pi_{b_{23}}^{(2,3)}$$

$$= \mathcal{N}_4 \sum_{cd} [F_{a_3 a_4}^{a_3 a_4}]_{hd} [F_c^{a_4 g a_4}]_{a_1 a_1} R_c^{a_4 a_1}$$

$$= \mathcal{N}_4 \sum_{cd} [F_{a_3 a_4}^{a_3 a_4}]_{hd} [F_c^{a_4 g a_4}]_{a_1 a_1} R_c^{a_4 a_1} \Pi_d^{(3,4)} \Pi_c^{(1,4)} \Pi_{b_{23}}^{(2,3)}.$$

$$\tag{11}$$

Equation (11) is applicable to models of either anyons or defects [40] which exhibit interesting projective non-Abelian statistics as long as the collective charges  $b_{23}, b_{12}, b_{24}$  and  $\tilde{b}_{23}$  are Abelian.

### 2.3. Effective braiding for parafermions

To dis-entangle the effective braiding from the charge transfers, we apply the result to the  $\mathbb{Z}_N$  parafermion model [6, 14] which is physically relevant ( $N = 2$  is the MF case). For  $\mathbb{Z}_N$  parafermions, there are  $N$  fusion states  $|q\rangle$  of two parafermions  $\sigma$ , where  $q = 0, \dots, N - 1$  is the Abelian charge (defined modulo  $N$ ). The  $F$ -matrix of parafermions is given by [19, 40, 46]

$$[F_b^{\sigma a \sigma}]_{\sigma\sigma} = \omega^{-ab}, \quad \omega = e^{\frac{i2\pi}{N}}, \quad (12)$$

where  $a$  and  $b$  are Abelian charges. Plugging equation (12) into equation (11), we have

$$\hat{M}_{14,23} \Pi_{b_{23}}^{(23)} = e^{i\phi} \sum_{cd} \omega^{hd-gc} R_c^{\sigma_4 \sigma_1} \Pi_d^{(34)} \Pi_c^{(14)} \Pi_{b_{23}}^{(23)}, \quad (13)$$

where  $\phi$  is an overall phase. In addition, the braiding and parity operators of parafermion modes  $\gamma_i$  and  $\gamma_j$  act on the fusion states in the following ways

$$\begin{aligned} \hat{R}_{ij}|q\rangle_{ij} &= R_q^{\sigma_i \sigma_j} |q\rangle_{ij}, \quad \hat{P}_{ij}|q\rangle_{ij} = \omega^q |q\rangle_{ij}, \\ \hat{P}_{ij} &= \omega^{\frac{N+1}{2}} \gamma_i^\dagger \gamma_j. \end{aligned} \quad (14)$$

Using equation (14), we can express equation (13) in operator form

$$\hat{M}_{14,23} \Pi_{b_{23}}^{(23)} = e^{i\phi} \sum_{cd} (\hat{P}_{34})^h \Pi_d^{(34)} (\hat{P}_{14})^{-g} \hat{R}_{14} \Pi_c^{(14)} \Pi_{b_{23}}^{(23)}. \quad (15)$$

Now, we supplement a correction operator  $\hat{C}_{14,23}^{g,h}$

$$\begin{aligned} \hat{C}_{14,23}^{g,h} [\hat{M}_{14,23} \Pi_{b_{23}}^{(23)}] &= e^{i\phi} \hat{R}_{14} \Pi_{b_{23}}^{(23)}, \\ \hat{C}_{14,23}^{g,h} &= (\hat{P}_{14})^g (\hat{P}_{34})^{-h}. \end{aligned} \quad (16)$$

It becomes apparent that the ancilla parafermions 2 and 3 return to their initialized collective charge state  $b_{23}$  and an effective braiding exchange is achieved between parafermions 1 and 4 (figure 1(e))

$$\hat{C}_{14,23}^{g,h} \hat{M}_{14,23} = e^{i\phi} \hat{R}_{14}. \quad (17)$$

Equation (17) is the central result of our paper and the key insight here is to undo the charge transfers occurred during the measurements to realize the desired braiding operation. Taking  $N = 2$ , equation (16) is consistent with our previous results of MFs [27] obtained using a wave-function approach.

## 3. How to apply the correction operator $\hat{C}$ ?

### 3.1. Hardware-implemented correction operator

In principle, it is possible to apply the correction operator  $\hat{C}$  in a topologically protected way on the hardware. For the special case of MFs, one possible approach is to use the Aharonov–Casher (AC) effect [47, 48]. The parity operator  $\hat{P}_{ij}$  is the Pauli  $\hat{\sigma}_z$  operator in the logical space of MFs  $\gamma_i$  and  $\gamma_j$ . Applying  $\hat{P}_{ij}$  imprints a  $\pi$ -phase difference between the logical state  $|0\rangle_{ij}$  and  $|1\rangle_{ij}$ . This can be achieved using the setup for the interferometry experiments proposed by Clarke and Shtengel [49], and Grosfeld and Stern [50]. The Majorana modes are hosted by the inner superconducting island using the Majorana wire approach [4, 5]. A Josephson vortex (fluxon) can be generated on demand in the circular Josephson junction and driven to circulate the loop by an applied supercurrent [48, 51–53]. Looping the fluxon around the inner superconducting island once will lead to a phase  $\pi Q/2e$  due to the AC effect [47, 48, 54], where  $Q$  is the charge on the island. Therefore, an exact  $\pi$ -phase difference will be produced between  $|0\rangle_{ij}$  and  $|1\rangle_{ij}$  states, which is equivalent to applying the parity operator.

### 3.2. Software-implemented correction operator

For quantum computation with  $\mathbb{Z}_N$  parafermions, we show that the correction operator can be applied in software to completely avoid potential errors introduced by the hardware approach, similar to how Pauli operations can be implemented in surface codes [55]. In particular, we consider the implementation of correction operators in software in three cases. Since braiding is the building block of TQC, we first show the case of how to implement correction operator in software for a set of two braidings. Next, we study the case of implementing correction operator in software for a braiding operation followed by a charge measurement. Those two cases form the building blocks for the third case of applying in software correction operators in a generic computation comprising Clifford gates and charge measurements.

### 3.2.1. Case A: two braidings

Suppose we want to implement a braiding operation  $\hat{R}_{i_1 i_4}$  to exchange computational parafermions  $i_1$  and  $i_4$  using ancilla parafermions  $i_2$  and  $i_3$ , which is followed by the braiding exchange  $\hat{R}_{j_1 j_4}$  of computational parafermions  $j_1$  and  $j_4$  using ancilla  $j_2$  and  $j_3$ . We consider general braidings, and hence computational parafermion  $i_1$  or  $i_4$  can be the same as  $j_1$  or  $j_4$ . The same holds for ancilla parafermions  $i_2, i_3, j_2$  and  $j_3$ . However, ancilla parafermions are solely used for assisting braiding and are different from computational parafermions. According to equation (17), these two braidings can be simulated by FMF-MBB protocol

$$\hat{R}_{j_1 j_4} \hat{R}_{i_1 i_4} = [\hat{C}_{j_1 j_4, j_2 j_3}^{g_j, h_j} \hat{M}_{j_1 j_4, j_2 j_3}] [\hat{C}_{i_1 i_4, i_2 i_3}^{g_i, h_i} \hat{M}_{i_1 i_4, i_2 i_3}], \quad (18)$$

where

$$g_k = b_{k_1 k_2} \times \bar{b}_{k_2 k_4}, \quad h_k = \bar{b}_{k_2 k_3} \times \bar{b}_{k_2 k_3}, \quad k = i, j, \quad (19)$$

keep track of intermediate charge transfers. Hereafter, we neglect the trivial overall phase factor. The TPM operator for parafermions is given by

$$\hat{M}_{k_1 k_4, k_2 k_3} = \prod_{\bar{b}_{k_2 k_3}}^{(k_2 k_3)} \prod_{b_{k_2 k_4}}^{(k_2 k_4)} \prod_{b_{k_1 k_2}}^{(k_1 k_2)}, \quad (20)$$

where the projective charge measurement of parafermions can be expressed in terms of the parity operator

$$\Pi_{b_{pq}}^{(pq)} = \sum_{\ell=1}^N (\omega^{-b_{pq}} \hat{P}_{pq})^\ell. \quad (21)$$

Parafermions obey the commutation relation

$$\gamma_p \gamma_q = \omega^{\text{sgn}(q-p)} \gamma_q \gamma_p, \quad (22)$$

where  $\text{sgn}(q - p)$  shows the importance of the relative ordering of  $\gamma_q$  and  $\gamma_p$  when  $\omega^{-1} \neq \omega$ .

Without loss of generality, we assume  $j_{1-4} \leq i_{1-4}$  in the relative ordering of parafermion modes. [14]. In this case, we can commute  $\hat{C}_{i_1 i_4, i_2 i_3}^{g_i, h_i}$  through  $\hat{M}_{j_1 j_4, j_2 j_3}$  using equation (22)

$$\hat{R}_{j_1 j_4} \hat{R}_{i_1 i_4} = \hat{C}_{j_1 j_4, j_2 j_3}^{g_j, h_j} \hat{C}_{i_1 i_4, i_2 i_3}^{g_i, h_i} \hat{M}'_{j_1 j_4, j_2 j_3} \hat{M}_{i_1 i_4, i_2 i_3}, \quad (23)$$

where

$$\hat{M}'_{j_1 j_4, j_2 j_3} = \prod_{\bar{b}'_{j_2 j_3}}^{(j_2 j_3)} \prod_{b'_{j_2 j_4}}^{(j_2 j_4)} \prod_{b'_{j_1 j_2}}^{(j_1 j_2)}, \quad (24)$$

$$b'_{j_1 j_2} = b_{j_1 j_2} + [\delta_{j_1 i_1} - \delta_{j_1 i_4}] g_i + [\delta_{j_1 i_4} + \delta_{j_2 i_3}] h_i, \quad (25)$$

$$b'_{j_2 j_4} = b_{j_2 j_4} + [\delta_{j_4 i_4} - \delta_{j_4 i_1}] g_i - [\delta_{j_4 i_4} + \delta_{j_2 i_3}] h_i, \quad (26)$$

$$\bar{b}'_{j_2 j_3} = \bar{b}_{j_2 j_3} + [\delta_{j_3 i_3} - \delta_{j_2 i_3}] h_i. \quad (27)$$

Here,  $g_i = b_{i_1 i_2} \times \bar{b}_{i_2 i_4}$  and  $h_i = \bar{b}_{i_2 i_3} \times \bar{b}_{i_2 i_3}$  are the charge transfers between parafermions  $i_1$ – $i_4$  expressed in terms of the charge readouts. To simplify the above expression, we introduce the short-hand notations

$$R_k \equiv \hat{R}_{k_1 k_4}, \quad C_k \equiv \hat{C}_{k_1 k_4, k_2 k_3}^{g_k, h_k}, \quad M_k \equiv \hat{M}_{k_1 k_4, k_2 k_3}, \quad (28)$$

$$\mathbf{b}_j = \begin{bmatrix} b_{j_1 j_2} \\ b_{j_2 j_4} \\ \bar{b}_{j_2 j_3} \end{bmatrix}, \quad \mathbf{b}'_j = \begin{bmatrix} b'_{j_1 j_2} \\ b'_{j_2 j_4} \\ \bar{b}'_{j_2 j_3} \end{bmatrix}. \quad (29)$$

The intermediate charge measurement results are implicitly in the short-hand notations, and we can express equations (24)–(27) as

$$R_j R_i = (C_j M_j) (C_i M_i) = C_j C_i M'_j M_i, \quad (30)$$

$$M'_j = \prod_{\bar{b}'_{j_2 j_3}}^{(j_2 j_3)} \prod_{b'_{j_2 j_4}}^{(j_2 j_4)} \prod_{b'_{j_1 j_2}}^{(j_1 j_2)}, \quad (31)$$

$$\mathbf{b}'_j = \mathbf{b}_j + \Delta_j(\mathbf{g}_i, \mathbf{h}_i), \quad (32)$$

where

$$\Delta_j(\mathbf{g}_i, \mathbf{h}_i) = \begin{bmatrix} (\delta_{j_1 i_1} - \delta_{j_1 i_4})\mathbf{g}_i + (\delta_{j_1 i_4} + \delta_{j_2 i_3})\mathbf{h}_i \\ (\delta_{j_4 i_4} - \delta_{j_4 i_1})\mathbf{g}_i - (\delta_{j_4 i_4} + \delta_{j_2 i_3})\mathbf{h}_i \\ (\delta_{j_3 i_3} - \delta_{j_2 i_3})\mathbf{h}_i \end{bmatrix} \quad (33)$$

is the difference between the charge measurement results before and after commuting  $C_i$  through  $M_j$ . It is dependent on the intermediate measurement results encoded in  $\mathbf{g}_i$  and  $\mathbf{h}_i$  from the first TPM operator, and that whether the two set of parafermions are the same or not. Therefore, the effect of postponing the correction operator is to have updated intermediate measurement results in the second TPM operator.

### 3.2.2. Case B: a braiding followed by a charge measurement

Next, we consider the case of a braiding operation  $R_i$  followed by a charge measurement  $\Pi_j$ .  $R_i$  realizes the braiding exchange between computational parafermions  $i_1$  and  $i_4$  assisted by the ancilla parafermions  $i_2$  and  $i_3$ . According to equation (17),  $R_i$  can be simulated by a TPM operator  $M_i$  followed by a correction operator  $C_i$ , where  $M_i \equiv \hat{M}_{i_1 i_4, i_2 i_3}$  and  $C_i \equiv \hat{C}_{i_1 i_4, i_2 i_3}^{g_i, h_i}$ . The charge measurement  $\Pi_j \equiv \Pi_{c_{j_1 j_4}}^{(j_1 j_4)}$  measures the collective charge  $c_{j_1 j_4}$  of computational parafermions  $j_1$  and  $j_4$ , which can be the same as  $i_1$  or  $i_4$  but not  $i_2$  and  $i_3$ . The operator for this case can be written as

$$\Pi_j R_i = \Pi_j (C_i M_i) = \Pi_{c_{j_1 j_4}}^{(j_1 j_4)} \hat{C}_{i_1 i_4, i_2 i_3}^{g_i, h_i} \hat{M}_{i_1 i_4, i_2 i_3}. \quad (34)$$

Again, we assume  $j_{1,4} \leq i_{1-4}$  in the relative ordering of parafermion modes. After commuting the correction operator through the charge measurement operator using equation (22), we have

$$\Pi_j R_i = \Pi_j (C_i M_i) = C_i \Pi'_j M_i, \quad (35)$$

where

$$\Pi'_j = \Pi_{c_{j_1 j_4}}^{(j_1 j_4)}, \quad (36)$$

$$c'_{j_1 j_4} = c_{j_1 j_4} + \eta_j(\mathbf{g}_i, \mathbf{h}_i), \quad (37)$$

$$\eta_j(\mathbf{g}_i, \mathbf{h}_i) = (\delta_{j_1 i_1} - \delta_{j_4 i_1})\mathbf{g}_i + (\delta_{j_4 i_4} - \delta_{j_1 i_4})(\mathbf{g}_i - \mathbf{h}_i), \quad (38)$$

encodes the change of the final measurement result due to commuting the correction operator through.

### 3.2.3. Case C: general computation

Now, for a general computation comprised of Clifford gates, we can break it down to a series of braiding operations  $R_i$ ,  $i = 1, \dots, m$ , followed by a set of final projective measurements  $\mathbf{\Pi} = (\Pi_1, \Pi_2, \dots, \Pi_n)$  on the logical qubits to extract information as shown in figure 2(a) (we defer the discussion of non-Clifford gates to next section). Here, each braiding operation involves two computational parafermions and two ancilla parafermions, and each charge measurement involves two computational parafermions. For simplicity, we keep the indices of the parafermions implicit in the definition of  $R_i$  and  $\mathbf{\Pi}$ .

According to equation (17), each braiding operation  $R_i$  can be simulated by a combination of a TPM operator  $M_i$  and a correction operator  $C_i$  as shown in figure 2(b). According to the discussion in section 3.2.1, we can commute  $C_{m-1}$  through  $M_m$ , which then becomes  $M'_m$ . In general, for  $M_i$  we need to commute  $C_1, \dots, C_{i-1}$  through and  $M_i$  becomes  $M'_i$  with a set of updated charge measurements

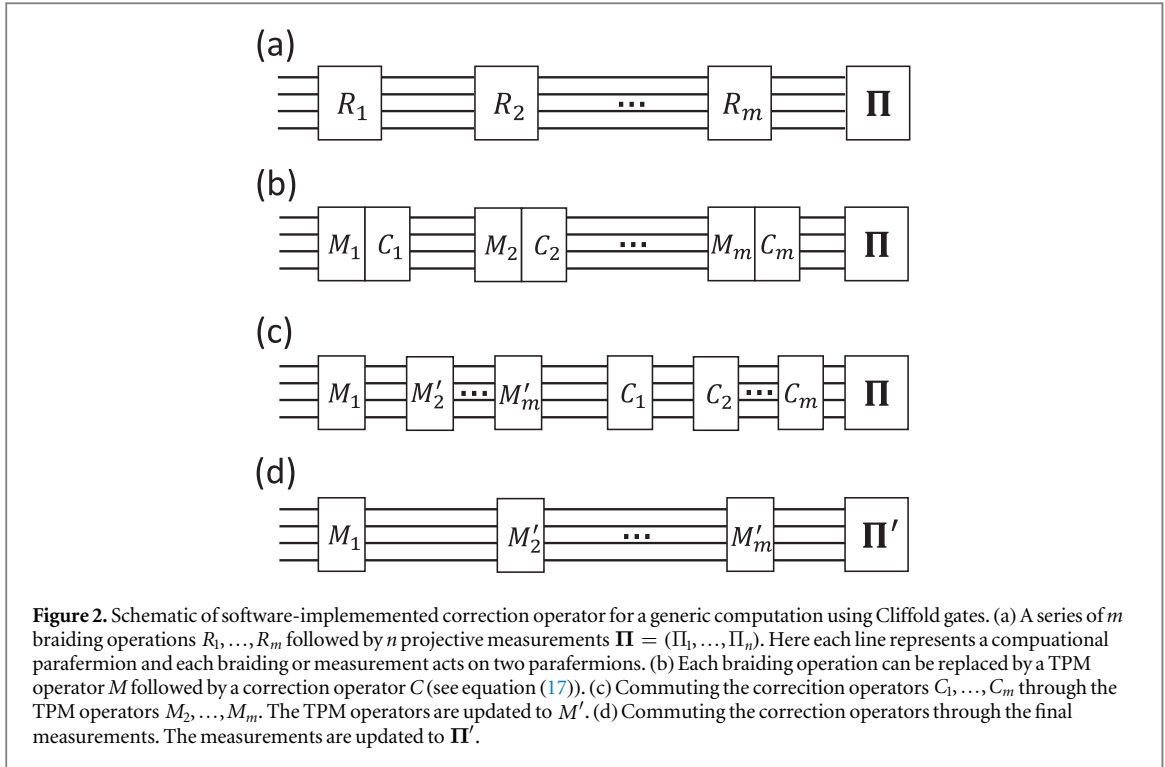
$$\mathbf{b}'_i = \mathbf{b}_i + \sum_{k=1}^{i-1} \Delta_i(\mathbf{g}_k, \mathbf{h}_k), \quad (39)$$

where  $\mathbf{b}_i$  is the set of charge measurements of  $M_i$  and  $\Delta_i(\mathbf{g}_k, \mathbf{h}_k)$  is defined in equation (32), encoding the change due to commuting  $C_k$  through<sup>3</sup>  $M_i$ . Figure 2(c) illustrates the impact of commuting all the correction operators through the TPM operators.

In the final step of software-implemented correction operator, we commute all the correction operators through the final set of logic measurements  $\mathbf{\Pi}$  following section 3.2.2. According to equations (35)–(38), charge measurement  $\Pi_j$  in  $\mathbf{\Pi}$  will become  $\Pi'_j$  with updated charge measurement result

$$c'_j = c_j + \sum_{k=1}^m \eta_j(\mathbf{g}_k, \mathbf{h}_k), \quad (40)$$

<sup>3</sup> The detailed form of  $\Delta_i(\mathbf{g}_k, \mathbf{h}_k)$  can be different from equation (32) where a particular ordering of parafermions is assumed.



where  $\eta_j(g_k, h_k)$  is defined in equation (38), encoding the change due to commuting  $C_k$  through  $\Pi_j$ . Once commuted through the final measurements, the correction operators have no impact on the computation any more. The final result of software-implemented correction operators is shown in figure 2(d).

Therefore, the general procedure for carrying out a computation in figure 2(a) is to follow the steps in figure 2(d) and record the charge measurement results  $(\mathbf{b}'_1, \dots, \mathbf{b}'_m)$  of the TPM operators as well as the final measurements  $(c'_1, \dots, c'_n)$ . In order to extract the actual logic measurement results  $(c_1, \dots, c_n)$ , we can do postprocessing in two steps. First, using equation (39) we can perform a backtracking to find  $(\mathbf{b}_1, \dots, \mathbf{b}_m)$ . For instance,  $\mathbf{b}_1$  is the same as  $\mathbf{b}'_1$ , which can be used to compute  $\Delta_2(g_1, k_1)$ . Then,  $\mathbf{b}_2$  can be calculated using  $\mathbf{b}'_2$  and  $\Delta_2(g_1, k_1)$ . For general  $i$ , we use all the previously calculated  $\mathbf{b}_1, \dots, \mathbf{b}_{i-1}$  to compute  $\Delta_i(g_k, h_k)$  ( $k = 1, \dots, i-1$ ), which is further used to find  $\mathbf{b}_i$ . This way, we can calculate  $(\mathbf{b}_1, \dots, \mathbf{b}_m)$  using  $(\mathbf{b}'_1, \dots, \mathbf{b}'_m)$ . The second step of postprocessing is to compute  $\eta_j(g_k, h_k)$  using  $(\mathbf{b}_1, \dots, \mathbf{b}_m)$ . Then equation (40) will give us the desired actual measurements  $(c_1, \dots, c_n)$ . We summarize the postprocessing backtracking algorithm below. It runs in linear time of the number of braiding operations and hence can be carried out efficiently. This is the essence of the software-assisted FMF MBB.

**Algorithm 1.** Postprocessing backtracking algorithm.

**Input:**  $(\mathbf{b}'_1, \dots, \mathbf{b}'_m)$ : intermediate charge measurements

$(c'_1, \dots, c'_n)$ : measured charges in the final measurement of  $\Pi'$  in figure 2(d)

**Output:**  $(c_1, \dots, c_n)$ : original measured charges in figure 2(a)

1:  $\mathbf{b}_1 = \mathbf{b}'_1 \rightarrow (g_1, k_1)$  (equation (19))

2: **for**  $i = 2$  to  $m$  **do**

3:  $g_{i-1}, k_{i-1} \rightarrow \Delta_i(g_{i-1}, k_{i-1})$  (equation (33))

4:  $\mathbf{b}'_i, \Delta_i(g_i, k_i), \dots, \Delta_i(g_{i-1}, k_{i-1}) \rightarrow \mathbf{b}_i$  (equation (39))

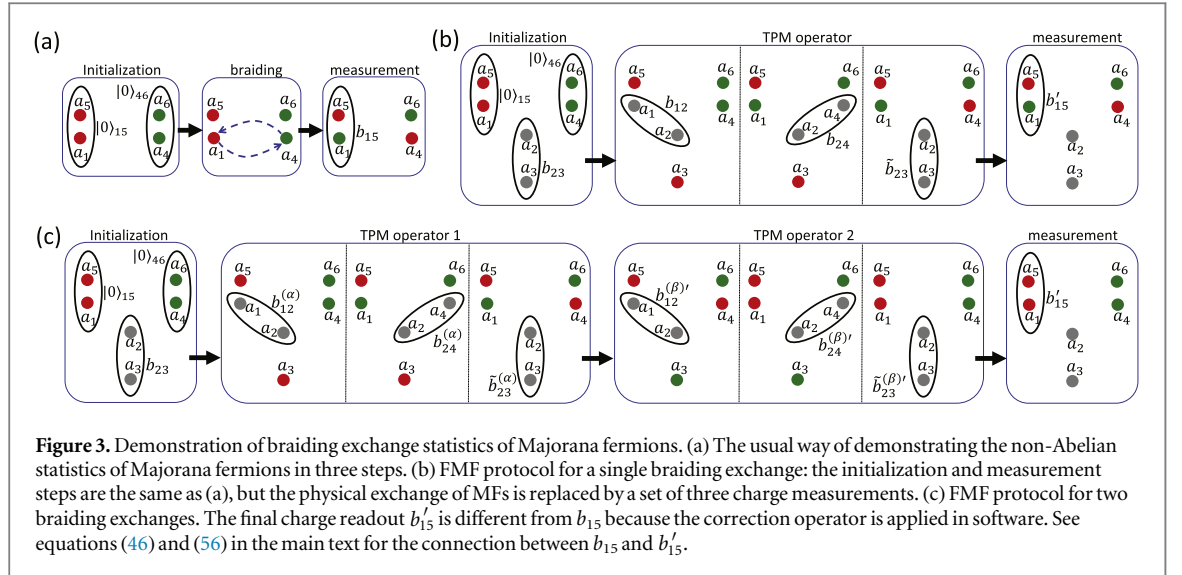
5:  $\mathbf{b}_i \rightarrow g_i, k_i$  (equation (19))

6:  $(g_1, h_1, \dots, g_m, h_m) \rightarrow \eta_j(g_i, h_i)$  (equation (38))

7: **for**  $j = 1$  to  $n$  **do**

8:  $c'_j, \eta_j(g_1, h_1), \dots, \eta_j(g_m, h_m) \rightarrow c_j$  (equation (40))

<sup>4</sup> Again, the detailed form of  $\eta_j(g_k, h_k)$  can be different from equation (38) where a particular ordering of parafermions is assumed.



## 4. Demonstration of non-Abelian statistics with FMF-MBB protocol

Now, we show how to apply our software-assisted FMF-MBB protocol to the task of demonstrating non-Abelian statistics of MFs. We do this by considering the two simplest examples of braiding experiments involving a single braiding exchange and two braiding exchanges.

### 4.1. Single-braiding experiment

Figure 3(a) shows the usual way of using a single braiding exchange to demonstrate non-Abelian statistics of MFs in three steps. First, Majorana pairs of (1, 5) and (4, 6) are initialized in the even parity states. Then MFs 1 and 4 are moved physically to exchange their positions [45]. Finally, the fermion charge  $b_{15}$  of the pair (1, 5) is measured. Ideally, the parity of  $b_{15}$  has 50% probability to be even or odd, which is a direct evidence of the non-Abelian statistics of MFs.

Figure 3(b) shows the approach of FMF-MBB using ancilla MFs  $a_2$  and  $a_3$ . We replace the physical exchange of MFs 1 and 4 by the software-assisted FMF-MBB which is followed by a final charge measurement of the pair (1, 5). The parity of  $b'_{15}$  can be different from that of  $b_{15}$ . The operator describing the usual braiding in figure 3(a) is given by

$$\hat{F}_1 = \Pi_{b_{15}}^{(15)} \hat{R}_{14}. \quad (41)$$

Using equation (17), we can replace the braiding operator by the set of three measurements shown in figure 3(b) followed by the correction operator (ignoring the trivial phase factor)

$$\hat{F}_1 = \Pi_{b_{15}}^{(15)} \hat{C}_{14,23}^{g,h} \hat{M}_{14,23}, \quad (42)$$

where

$$g = b_{12} \otimes \bar{b}_{24}, \quad (43)$$

$$h = \bar{b}_{23} \otimes \bar{b}_{23}. \quad (44)$$

After commuting the correction operator through the final charge measurement, we have

$$\hat{F}_1 = \hat{C}_{14,23}^{g,h} \Pi_{b'_{15}}^{(15)} \hat{M}_{14,23}, \quad (45)$$

where

$$b'_{15} = b_{15} + g. \quad (46)$$

Therefore, for the single braiding experiment, one just needs to follow the steps depicted in figure 3(b) and the actual charge  $b_{15}$  is connected to the measured charged  $b'_{15}$  via equation (46).

### 4.2. Double-braiding experiment

The case of two braidings can be approached in a similar way as shown in figure 3(c). The operator describing the action of two braiding exchanges followed by a charge readout is given by

$$\hat{F}_2 = \Pi_{b_{15}}^{(15)} \hat{R}_{14}^{(\beta)} \hat{R}_{14}^{(\alpha)}. \quad (47)$$

Using equation (17), we have (again, neglecting the overall phase factor)

$$\hat{F}_2 = \Pi_{b_{15}}^{(15)} [\hat{C}_{14,23}^{g_\beta, h_\beta} \hat{M}_{14,23}^{(\beta)} [\hat{C}_{14,23}^{g_\alpha, h_\alpha} \hat{M}_{14,23}^{(\alpha)}], \quad (48)$$

where  $\hat{M}_{14,23}^{(\alpha)}$  and  $\hat{M}_{14,23}^{(\beta)}$  are the first and second TPM operators respectively and

$$g_{\alpha,\beta} = b_{12}^{(\alpha,\beta)} \otimes \bar{b}_{24}^{(\alpha,\beta)}, \quad (49)$$

$$h_{\alpha,\beta} = \tilde{b}_{23}^{(\alpha,\beta)} \otimes \bar{b}_{23}^{(\alpha,\beta)}. \quad (50)$$

Finally, we can commute the two correction operators through the final charge measurement operator (equation (23) and equation (45))

$$\hat{F}_2 = \hat{C}_{14,23}^{g_\beta, h_\beta} \hat{C}_{14,23}^{g_\alpha, h_\alpha} \Pi_{b_{15}}^{(15)} \hat{M}_{14,23}^{(\beta)'} \hat{M}_{14,23}^{(\alpha)}, \quad (51)$$

where

$$\hat{M}_{14,23}^{(\beta)'} = \Pi_{\tilde{b}_{23}}^{(23)} \Pi_{b_{24}}^{(24)} \Pi_{b_{12}}^{(12)}, \quad (52)$$

$$b_{12}^{(\beta)'} = b_{12}^{(\beta)} + g_\alpha, \quad (53)$$

$$b_{24}^{(\beta)'} = b_{24}^{(\beta)} + g_\alpha - h_\alpha, \quad (54)$$

$$\tilde{b}_{23}^{(\beta)'} = \tilde{b}_{23}^{(\beta)} + h_\alpha, \quad (55)$$

$$b_{15}' = b_{15} + g_\alpha + g_\beta. \quad (56)$$

In the two braiding experiment using our proposed FMF-MBB protocol, we have access to the charge readouts  $b^{(\alpha)}$  from the first set of three measurements,  $b^{(\beta)'}$  from the second set, and the final charge readout  $b_{15}'$ . We can first backtrack and calculate  $b^{(\beta)}$  using equations (53)–(55), which yields  $g_\beta$  and  $h_\beta$  according to equations (49) and (50). Then a further backtracking using equation (56) gives us the actual parity of  $b_{15}$  after two braiding exchanges. Here, the key is that the correction operator is a Pauli operator acting on the logical qubit made of two Majorana modes. The TPM operator comprises three single-qubit projective measurements, which remain projective measurements with updated measurement results after commuting Pauli operators through.

Ideally, given an initially even parity state of (1, 5),  $b_{15}$  has a 100% probability of flipping to the odd parity after two braidings as a direct consequence of the non-Abelian statistics of MFs. Here, the only experimental capability required is to perform quantum non-demolition (QND) readouts of the charge of Majorana pairs [45, 54]. Such a simplification will allow us not to worry about the diabatic errors associated with moving MFs and instead to concentrate on improving readout techniques. In fact, because the measurements are QND, a natural way to boost the measurement fidelity is to simply repeat the same charge readout several times. In addition, FMF-MBB protocol removes the uncertainty associated with the number of measurements in the original MBB approach, and hence is more efficient experimentally. Therefore, we believe our FMF-MBB approach can be an appealing avenue to the demonstration of non-Abelian braiding statistics.

## 5. MOTQC with FMF-MBB protocol

Finally, we outline how to adapt our FMF protocol to the more ambitious long-term goal of MOTQC using MFs and parafermions. For Clifford gates, it is straightforward to apply the software-assisted FMF-MBB protocol because braiding itself is enough to carry out Clifford operations.

However, to complete the set of gates for universal quantum computation using MFs, one also needs to add the  $\pi/8$ -phase gate ( $\hat{T}$  gate) which cannot be realized in a topologically protected way. Fortunately, there exist protocols such as ‘magic state distillation’ to generate a high fidelity  $\hat{T}$  gate. First, the distillation protocol starts with 15 approximate copies of the ancilla state  $|a\rangle = (|0\rangle + e^{i\pi/4}|1\rangle)/\sqrt{2}$ . For MFs, this can be done by initializing the state in  $|0\rangle$  and performing a single-qubit  $\pi/4$  rotation. One way to generate the single-qubit rotation is to bringing two Majorana modes together for a fixed amount of time such that the tunneling splitting imposes an approximate  $\pi/4$  phase difference between  $|0\rangle$  and  $|1\rangle$ . Another possibility is to use hybrid systems that couple the MFs with other physical devices (e.g., tunnel junctions, flux qubits) to produce the desired ancillary states [49, 54, 56–58]. In the second step, these states are then projected onto the subspace of the Reed-Muller code [59, 60]. By subsequent stabilizer measurements, the states are encoded into a single logical qubit and it is a purified version of  $|a\rangle$ . Finally, a  $T$  gate can be applied to the data qubit after performing several

Clifford operations and projective measurements on a small circuit made of the purified  $|a\rangle$  state and the data qubit<sup>5</sup>.

Notice that the first step to generate ancilla states is independent of how we carry out the braiding operations (no matter it is done via physical movements or our FMF-MBB protocol). However, the second and third steps do heavily depend on the details of braiding since all the Clifford operations break down to sequences of braiding exchanges. Fortunately, *there are only two types of operations in the distillation protocol, namely Clifford operations and single-qubit projective measurements*. Adopting the FMF-MBB protocol developed above, we can replace each braiding operator by the product of the TPM operator  $\hat{M}$  and the correction operator  $\hat{C}$  (equation (17)). All the correction operators can then be commuted through the final measurements (equation (51)). The single-qubit projective measurements remain Pauli measurements with updated measurement results dependent on the correction operators. Therefore, the same software-assisted FMF-MBB procedure outlined for the single-braiding and two-braiding experiments applies equally well to the magic state distillation protocol and hence to MOTQC using MFs.

For  $\mathbb{Z}_N$  parafermions, magic state distillation is well-studied for the case of prime  $N$  [61], and it was recently shown that all Clifford operations can be realized via braiding for odd  $N$  [62]. Hence, all the above discussion carries over to the scenario of TQC using odd prime  $N$  parafermions.

## 6. Conclusion

We have proposed a protocol of MBB without forced measurements. In particular, the braiding exchange is shown to be equivalent to a set of three measurements followed by a correction operation because we can always introduce correction operations to compensate the (topological) charge transfer during the MBB. Furthermore, for quantum computation with MFs or parafermions, we also show that the correction operator can be applied in software similar in spirit to how the Pauli operations can be implemented in surface codes. Like the original MBB protocol, our FMF-MBB protocol removes the need for moving anyons physically and reduces the experimental requirement of braiding to the capability of performing projective measurements only. Compared to the MBB protocol, it also removes the ambiguity in the number of measurements needed to realize a single braiding operation. Finally, we show explicitly that such a simple braiding protocol can be applied to both the demonstration of non-Abelian braiding statistics and measurement-based TQC using MFs and parafermions.

## Acknowledgments

We would like to thank Jukka Vayrynen, Aris Alexandradinata and Bernard van Heck for useful discussions. We acknowledge support from ARL-CDQI, ARO, AFOSR MURI, the Alfred P Sloan Foundation, and the Packard Foundation.

## References

- [1] Nayak C, Simon S H, Stern A, Freedman M and Sarma S Das 2008 *Rev. Mod. Phys.* **80** 1083
- [2] Stern A and Lindner N H 2013 *Science* **339** 1179
- [3] Kitaev A Y 2001 *Phys.-Usp.* **44** 131
- [4] Lutchyn R M, Sau J D and Sarma S Das 2010 *Phys. Rev. Lett.* **105** 077001
- [5] Oreg Y, Refael G and von Oppen F 2010 *Phys. Rev. Lett.* **105** 177002
- [6] Alicea J and Fendley P 2016 *Annu. Rev. Condens. Matter Phys.* **7** 119
- [7] Mourik V, Zuo K, Frolov S M, Plissard S R, Bakkers E P A M and Kouwenhoven L P 2012 *Science* **336** 1003
- [8] Das A, Ronen Y, Most Y, Oreg Y, Heiblum M and Shtrikman H 2012 *Nat. Phys.* **8** 887
- [9] Rokhinson L P, Liu X and Furdyna J K 2012 *Nat. Phys.* **8** 795
- [10] Deng M T, Yu C L, Huang G Y, Larsson M, Caroff P and Xu H Q 2012 *Nano Lett.* **12** 6414
- [11] Finck A D K, Van Harlingen D J, Mohseni P K, Jung K and Li X 2013 *Phys. Rev. Lett.* **110** 126406
- [12] Nadj-Perge S, Drozdov I K, Li J, Chen H, Jeon S, Seo J, MacDonald A H, Bernevig B A and Yazdani A 2014 *Science* **346** 6209
- [13] Albrecht S M, Higginbotham A P, Madsen M, Kuemmeth F, Jespersen T S, Nygard J, Krogstrup P and Marcus C M 2016 *Nature* **531** 206
- [14] Fendley P 2012 *J. Stat. Mech.* **P11020**
- [15] Barkeshli M and Qi X-L 2012 *Phys. Rev. X* **2** 031013
- [16] Lindner N H, Berg E, Refael G and Stern A 2012 *Phys. Rev. X* **2** 041002
- [17] Cheng M 2012 *Phys. Rev. B* **86** 195126
- [18] Clarke D J, Alicea J and Shtengel K 2013 *Nat. Commun.* **4** 1348
- [19] Vaezi A 2013 *Phys. Rev. B* **87** 035132
- [20] Barkeshli M and Qi X-L 2014 *Phys. Rev. X* **4** 041035
- [21] Oreg Y, Sela E and Stern A 2014 *Phys. Rev. B* **89** 115402
- [22] Klinovaja J, Yacoby A and Loss D 2014 *Phys. Rev. B* **90** 155447

<sup>5</sup> See figure 33 and section XVI of [55] for a detailed description.

- [23] Klinovaja J and Loss D 2014 *Phys. Rev. Lett.* **112** 246403
- [24] Bombin H 2010 *Phys. Rev. Lett.* **105** 030403
- [25] You Y-Z and Wen X-G 2012 *Phys. Rev. B* **86** 161107
- [26] Brown B J, Bartlett S D, Doherty A C and Barrett S D 2013 *Phys. Rev. Lett.* **111** 220402
- [27] Zheng H, Dua A and Jiang L 2015 *Phys. Rev. B* **92** 245139
- [28] Stoudenmire E M, Clarke D J, Mong R S K and Alicea J 2015 *Phys. Rev. B* **91** 235112
- [29] Barkeshli M and Sau J D 2015 Physical architecture for a universal topological quantum computer based on a network of Majorana nanowire (arXiv:1509.07135)
- [30] Knapp C, Zaletel M, Liu D E, Cheng M, Bonderson P and Nayak C 2016 *Phys. Rev. X* **6** 041003
- [31] van Heck B, Akhmerov A R, Hassler F, Burrello M and Beenakker C W J 2012 *New J. Phys.* **14** 035019
- [32] Burrello M, van Heck B and Akhmerov A R 2013 *Phys. Rev. A* **87** 022343
- [33] Bonderson P, Freedman M and Nayak C 2008 *Phys. Rev. Lett.* **101** 010501
- [34] Wootton J R 2005 *J. Phys. A: Math. Theor.* **48** 215302
- [35] Hutter A, Wootton J R and Loss D 2015 *Phys. Rev. X* **5** 041040
- [36] Bonderson P 2013 *Phys. Rev. B* **87** 035113
- [37] Kitaev A 2006 *Ann. Phys.* **321** 2
- [38] Bonderson P and 2007 Non-Abelian anyons and interferometry *PhD Thesis* California Institute of Technology
- [39] Bonderson P, Shtengel K and Slingerland J K 2008 *Ann. Phys.* **323** 47
- [40] Barkeshli M, Bonderson P, Cheng M and Wang Z 2014 Symmetry, defects, and gauging of topological phases (arXiv:1410.4540)
- [41] Das Sarma S, Freedman M and Nayak C 2005 *Phys. Rev. Lett.* **94** 166802
- [42] Stern A and Halperin B I 2006 *Phys. Rev. Lett.* **96** 016802
- [43] Bonderson P, Kitaev A and Shtengel K 2006 *Phys. Rev. Lett.* **96** 016803
- [44] van Heck B, Burrello M, Yacoby A and Akhmerov A R 2013 *Phys. Rev. Lett.* **110** 086803
- [45] Aasen D *et al* 2016 *Phys. Rev. X* **6** 031016
- [46] Barkeshli M, Jian C-M and Qi X-L 2013 *Phys. Rev. B* **87** 045130
- [47] Aharonov Y and Casher A 1984 *Phys. Rev. Lett.* **53** 319
- [48] Friedman J R and Averin D V 2002 *Phys. Rev. Lett.* **88** 050403
- [49] Clarke D J and Shtengel K 2010 *Phys. Rev. B* **82** 180519
- [50] Grosfeld E and Stern A 2011 *Proc. Natl Acad. Sci. USA* **108** 11810
- [51] Ustinov A V 2002 *Appl. Phys. Lett.* **80** 3153
- [52] Wallraff A, Lukashenko A, Lisenfeld J, Kemp A, Fistul M V, Koval Y and Ustinov A V 2003 *Nature* **425** 155
- [53] Beck M, Goldobin E, Neuhaus M, Siegel M, Kleiner R and Koelle D 2005 *Phys. Rev. Lett.* **95** 090603
- [54] Hassler F, Akhmerov A R, Hou C-Y and Beenakker C W J 2010 *New J. Phys.* **12** 125002
- [55] Fowler A G, Mariantoni M, Martinis J M and Cleland A N 2012 *Phys. Rev. A* **86** 032324
- [56] Bonderson P, Clarke D J, Nayak C and Shtengel K 2010 *Phys. Rev. Lett.* **104** 180505
- [57] Jiang L, Kane C L and Preskill J 2011 *Phys. Rev. Lett.* **106** 130504
- [58] Bonderson P and Lutchyn R M 2011 *Phys. Rev. Lett.* **106** 130505
- [59] Raussendorf R, Harrington J and Goyal K 2006 *Ann. Phys.* **321** 2242
- [60] Bravyi S and Kitaev A 2005 *Phys. Rev. A* **71** 022316
- [61] Campbell E T, Anwar H and Browne D E 2012 *Phys. Rev. X* **2** 041021
- [62] Hutter A and Loss D 2016 *Phys. Rev. B* **93** 125105